CHAPTER 184

Numerical Modeling of the Dredged Spoil Disposal

Cao Zude[1] Wang Guifen[2]

Abstract

To calculate the sediment movement under waves and currents, a simulating system called CW system has been developed by the authers. It can determine the effect of the dredged spoil disposal.

1 Introduction

Under the interaction of the wind wave and the tidal current some fluid mud and sediment suspension caused by dredged spoil disposal transport and flow complicatedly. Its propotion varies with the hydragraphic conditions.

We have measured the movement of the fluid mud by using "Neutron activation" and have developed a series of 2–dimensional and 3–dimensional numerical models to simulate the movement of suspended load, the fluid mud and their transformation by using the moving ADI method (Chen and Cao, 1990)

By field data, spoil materials were casted into the sea area, 70～90% of which were fluid mud on the bottom and 10～30% suspended load.

The fluid mud flows along the bottom by gravity、 wave and current. The suspended load moves with water. Both fluid mud and suspension deposit by and by. Some times in case of strong

---

1. Associate research fellow of coastal and estuary engineering, Tianjin Research Institute of Water Transport Engineering, Xingang, Tanggu, Tianjin, P.O.300456, China

2. Engineer of coastal and Estuary Engineering. Tianjin Research Institute of Water Transport Engineering, Xingang, Tanggu, Tianjin, P.O.300456, China

wind–wave the fluid mud becomes suspended. When the sea is calm the suspended load turns into the fluid mud.

The process is shown in Fig.1 as follows.

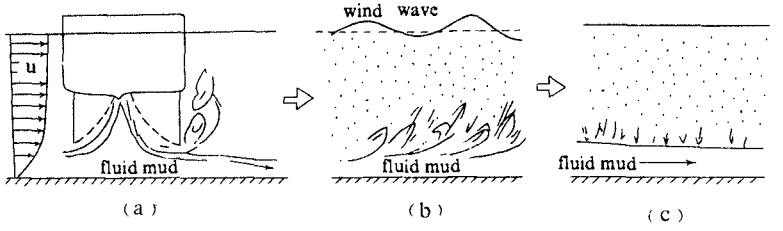

Fig. 1 Movement of dredged materials

Numerical modelling of the processes are shown in the Fig.1 of appendices.

2 Basic differencial equations

2–1 Tidal current

2–1–1 Two dimensional eguations (Cao et al.,1989)

In case of no wind

$$\frac{\partial \zeta}{\partial t}+\frac{\partial}{\partial x}(uh)+\frac{\partial}{\partial y}(vh)=0$$

$$\frac{\partial u}{\partial t}+u\frac{\partial u}{\partial x}+v\frac{\partial u}{\partial y}+g\frac{\partial \zeta}{\partial x}+\frac{gu\sqrt{u^2+v^2}}{c^2h}-fv=A\Delta u$$

$$\frac{\partial v}{\partial t}+v\frac{\partial u}{\partial y}+u\frac{\partial v}{\partial x}+g\frac{\partial \zeta}{\partial y}+\frac{gv\sqrt{u^2+v^2}}{c^2h}+fu=A\Delta v$$

In case of wind–wave

$$\frac{\partial \zeta}{\partial t}+\frac{\partial}{\partial x}(uh)+\frac{\partial}{\partial y}(vh)=0$$

$$\frac{\partial u}{\partial t}+u\frac{\partial u}{\partial x}+v\frac{\partial u}{\partial y}+g\frac{\partial \zeta}{\partial x}-fv-\frac{c_s\rho_a}{h\rho}|W-U|(\omega_x-u)$$

$$+\frac{1}{h}\frac{\tau_x}{\rho}+\frac{1}{\rho h}\left(\frac{\partial S_{xx}}{\partial x}+\frac{\partial S_{xy}}{\partial y}\right)=A\Delta u$$

$$\frac{\partial v}{\partial t}+u\frac{\partial v}{\partial x}+v\frac{\partial v}{\partial y}+g\frac{\partial \zeta}{\partial x}+fu-\frac{c_s\rho_a}{h\rho}\mid W-U\mid\ (\omega_y-v)$$

$$+\frac{\tau_y}{\rho h}+\frac{1}{\rho h}\left(\frac{\partial s_{yx}}{\partial x}+\frac{\partial s_{yy}}{\partial y}\right)=A\Delta v$$

2–1–2 Three dimensional eguations (Cao et al., 1988)

$$\frac{\partial \zeta_k}{\partial t}-\frac{\partial \zeta_{k-1}}{\partial t}+\frac{\partial\ (u_k h_k)}{\partial x}+\frac{\partial\ (v_k h_k)}{\partial y}=0$$

$$\frac{\partial h_k}{\partial t}=-\frac{\partial u_k h_k}{\partial x}-\frac{\partial v_k h_k}{\partial y}$$

$$\frac{\partial u_k}{\partial t}+u_k\frac{\partial u_k}{\partial x}+v_k\frac{\partial u_k}{\partial y}+\omega_k\frac{\partial u_k}{\partial z}+g\frac{\partial\ (\zeta_k-\zeta_{k-1})}{\partial x}-fv_k+\frac{1}{\rho h_k}$$

$$\times(\tau_{xk-1}-\tau_{xk})=A_x\Delta u_k$$

$$\frac{\partial v_k}{\partial t}+u_k\frac{\partial v_k}{\partial x}+v_k\frac{\partial v_k}{\partial y}+\omega_k\frac{\partial v_k}{\partial z}+g\frac{\partial\ (\zeta_k-\zeta_{k-1})}{\partial y}+fu_k$$

$$+\frac{1}{\rho h_k}(\tau_{yk-1}-\tau_{yk})=A_y\Delta v_k$$

2–2 Wave

The wave forecast and refraction are used in the CW system

2–3 The dispersion equations of suspended load

In case of 2–D (Cao et al., 1989)

$$\frac{\partial}{\partial t}(sh)+\frac{\partial}{\partial x}(suh)+\frac{\partial}{\partial y}(svh)+Fs=\frac{\partial}{\partial x}\left(D_x h\frac{\partial s}{\partial y}\right)$$

$$+\frac{\partial}{\partial y}\left(D_y h\frac{\partial s}{\partial y}\right)$$

In case of 3–D (Cao et al., 1988)

$$\frac{\partial}{\partial t}(s_k h_k) + \frac{\partial}{\partial x}(u_k s_k h_k) + \frac{\partial}{\partial y}(v_k s_k h_k) + (\omega - \omega_s) \times$$

$$s\Big|_{z_{k-1}}^{z_k} - \varepsilon_z \frac{\partial s}{\partial z}\Big|_{z_{k-1}}^{z_k} = \frac{\partial}{\partial x}(k_x h_k \frac{\partial s_k}{\partial x}) + \frac{\partial}{\partial y}(k_y h_k \frac{\partial s}{\partial y})$$

2–4 The fluid mud movement eguations. (Cao et al., 1988,1989).

$$\frac{\partial h_m}{\partial t} + \frac{\partial}{\partial x}(u_m h_m) + \frac{\partial}{\partial y}(v_m h_m) + F_s + F_b + F_c = 0$$

$$\frac{\partial u_m}{\partial t} + u_m \frac{\partial u_m}{\partial x} + v_m \frac{\partial u_m}{\partial y} + g\frac{\rho}{\rho_m}\frac{\partial \zeta}{\partial x} + g\frac{\Delta\rho}{\rho_m}\frac{\partial \zeta_m}{\partial x} +$$

$$\frac{1}{\rho_m h_m}(\tau_{bx} + \tau_{Bx} - \tau_x) = D_m \Delta u_m$$

$$\frac{\partial v_m}{\partial t} + u_m \frac{\partial v_m}{\partial x} + v_m \frac{\partial v_m}{\partial y} + g\frac{\rho}{\rho_m}\frac{\partial \zeta_m}{\partial y} + g\frac{\Delta\rho}{\rho_m}\frac{\partial \zeta_m}{\partial y} +$$

$$\frac{1}{\rho_m h_m}(\tau_{by} + \tau_{By} - \tau_y) = D_m \Delta v_m$$

2–5 Morphology

$$\frac{\partial \zeta_b}{\partial t} = F_s / \gamma_c$$

where ζ is the vertical displacement between the water level and the still water level;u,v,w are respectively compenent velocities in x.y and z directions; h–the water depth; f–Coriolis acceleration; H–the wave height; L–the wave length; C–the wave velocity; S–the concentration of suspended load; F_s–the Function of siltation and deposition; S_{xx}, S_{xy},$S_{yx}$and S_{yy}–the radiational stress; τ_b–the shear stress on bottom; τ_ω–the shear stress on surface by wind; τ_B–Bingham stress; and footnote "K"—the K–layer on 3–D; footnote "m"—fluid mud; footnote "b"—sea bottom.

These differential eguations mentioned above can be solved by the determined boundary conditions and initial conditions.

3 Applications (for example)

3–1 Computational regions

Based on these differential eguations mentioned above the simulating system called CW system has been developed by the writers in Tianjin Research Institute of Water Transport Engineering, China.

The CW System has been used to study the effects of the dredged spoil disposal on the environment and siltation in Tianjin Port.

As there is lack of boundary condition required in numerical simulations in Tianjin Port Area, 4 calculational regions with different ranges are set up by using the method of nesting small model in a large one. Bohai Sea is the first calculational region; Bohaiwan Bay–the second; The Tianjin Harbour Area–the third and the spoil ground—the fourth. These four regions are nested with each other.

The calculated results of the former regions provide the boundary conditions for the latter. The open boundary conditions of the first region are controlled by M_2, S_2, K_1, O_1 component tides.

Table 1 characteristics of calculation regions

no.	1	2	3	4
name	Bohai Sea	Bohai Bay	north part of Bohai Bay	dredged spoil ground
area(km^2)	168,000	10,800	5,400	25
simulation method	moving ADI method	moving ADI method	moving ADI method	explicit method
dimension	2	2	2	3
space step				
$\triangle x$ (m)	10,000	5,000	500	500
$\triangle y$ (m)	10,000	5,000	500	500
$\triangle z$ (m)				2
time step (s)	1,800	900	90	90

As contracted by the storage capacity, two dimensional modellings are used for the former three regions by means of "moving ADI method". and three dimensional modelling is used for the fourth region with explicit method. The "moving ADI method"

not only remains ADI method's characteristics but also has following advantages—fast in convergence; high in stability; simple in calculation and convenient in programing (Wang,1989).

The pictures of four calculational regions mentioned above are shown in Fig.2 and the technical functions of these regions are listed in table 1.

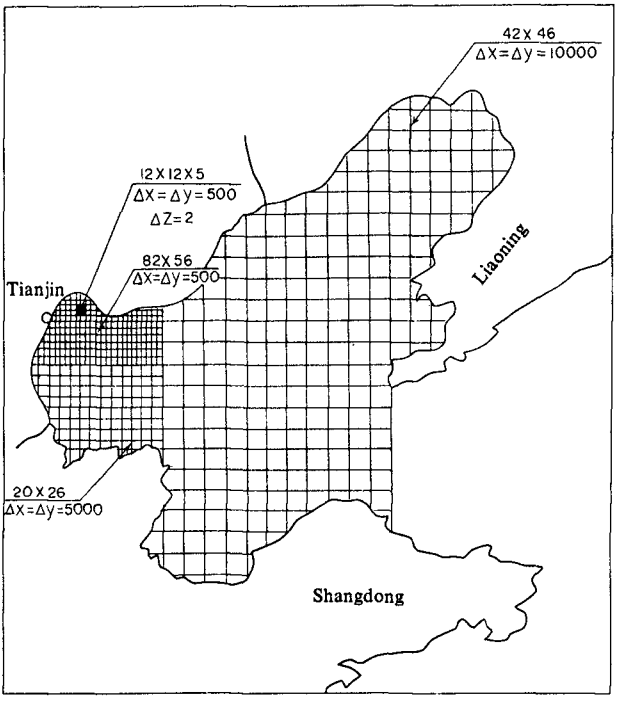

Fig. 2 Diagram of each calculation network

3–2 Verification

Five aspects are verified for these numerical modelling. The computational results agree well with the field data as follows.

3–2–1 Water level

The water level process at the center of spoil ground in spring tide on Aug. lst 1988 is shown in Fig 3.

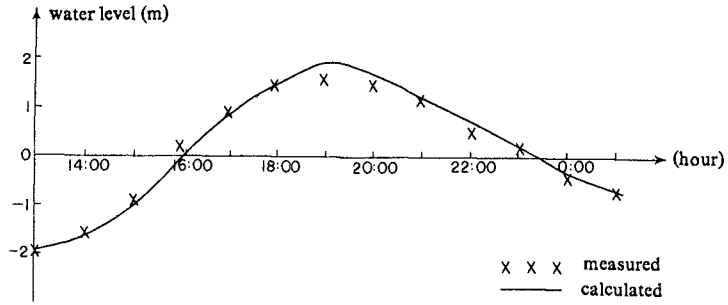

Fig. 3 Varification of water level process of spoil ground

3—2—2 Velocity

The velocity processes of five stations on the spoil ground during spring tide on Aug. lst of 1988 are shown in Fig.4.

The velocity processes of the four stations in both side of the channel during spring tide on Aug.lst , 1988 are shown in Fig. 5

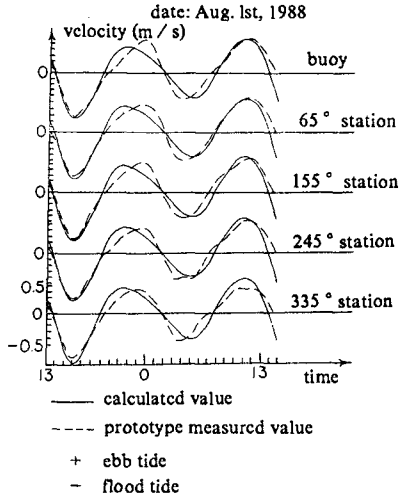

Fig. 4 Verification of current velocity process of spoil ground

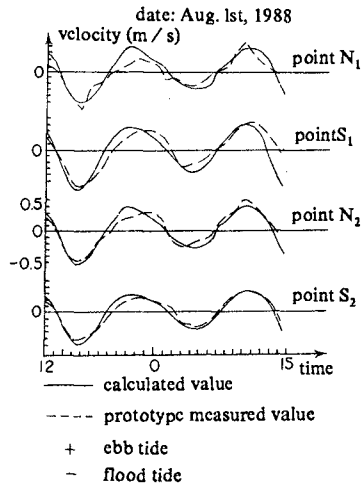

Fig. 5 Verification of current velocity of measuring stations to the south and north of the channel

The velocity distributions of velocity on the Aug. lst 1988 in the center of the spoil ground at different time are shown in Fig. 6.

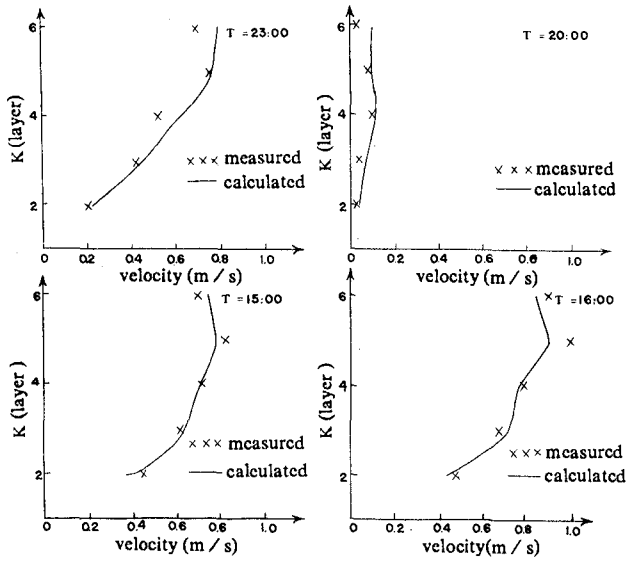

Fig. 6 Vertical distribution of current velocity of spoil ground

3–2–3 Tracing floats

Tracing floats from the center of the spoil ground at the flood tide and ebb tide are shown in Fig.7.

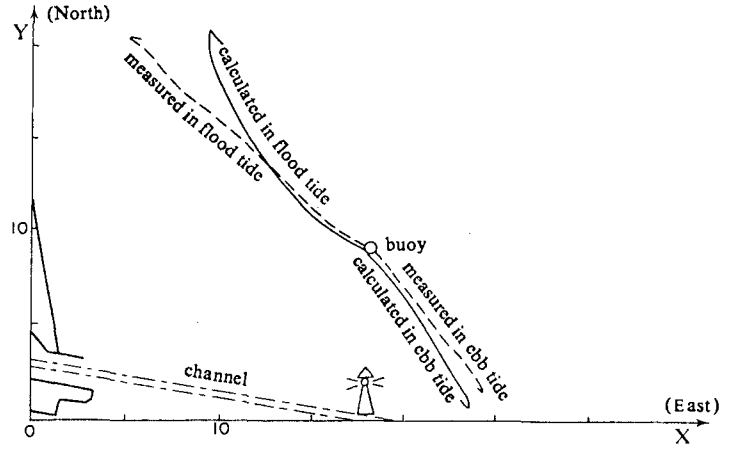

Fig. 7 Diagram of flow tracks of flood tide and ebb tide

3–2–4 Concentration of suspended load

The vertical distributions of concentration of suspended load in the center of the spoil ground at different time are shown in Fig. 8.

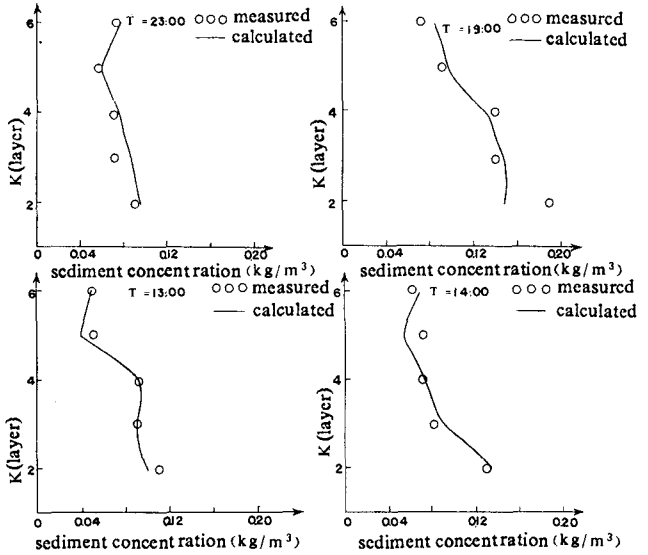

Fig. 8 Verification of vertical distribution of suspended sediment concentration at different times

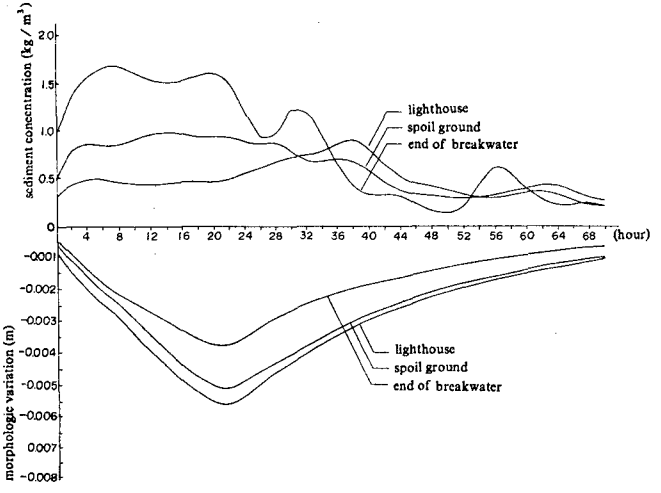

Fig. 9 Prcoess curves of sediment concentration and morphologic erosion

3–2–5 Morphologic processes.

Sediment concentration and morphologic variation of 3 locations (the entrance of Tianjin port, near the lighthouse and the center of spoil ground) under the action of the northeast gale are shown in Fig 9.

The simulated results are in good agreement with the measured in field.

3–3 Simulation of dredged materials

The dredged materials are disposed to the spoil ground with the self–propelled trailling suction hopper dredger as follows:

1.Disposing one boat of spoil materials;

2.Disposing a boat of spoil materials continuously at the interval of every two hours a week.

3. Simulating the effects of wind–wave process on the movement of spoil materials. The following simulated results are obtained:

The variation suspension and fluid mud under the effect of the northeast gale are shown in Fig 2 and 3 of appendices.

It is inticated from Fig 2～3 of appendices that the dredged materials on the existed spoil ground have no dirct effect on the siltation of Tianjin Port.

4 Conclutions

By comparing the simulated value and the field data we believe the CW system is an effective tool to study the movement of the spoil disposal

Reference

(1)Cao Zude, Wang Guifen, Zhang Yingping, 1988, Three Dimensional Numerical Modelling of Tidal Current and its Applications, Rep. of TRIWTE No. 8811.

(2) Cao Zude, Wang Guifen, Xu Hongming, Zhang Yinping, 1989, Numerical Simulation of Spoil Disposal on the Spoil Ground, Rep. of TRIWTE No. 8909.

(3) Chen Shengliang, Cao Zude, 1990, Effect of Dredged Spoil Materials on Siltation of Tianjin Port, Rep of TRIWTE No. 8912,

(4)Wan Guifen, 1989, A New Calculation Method—Moving ADI Method, Rep of TRIWTE No. 8911.

Appendices

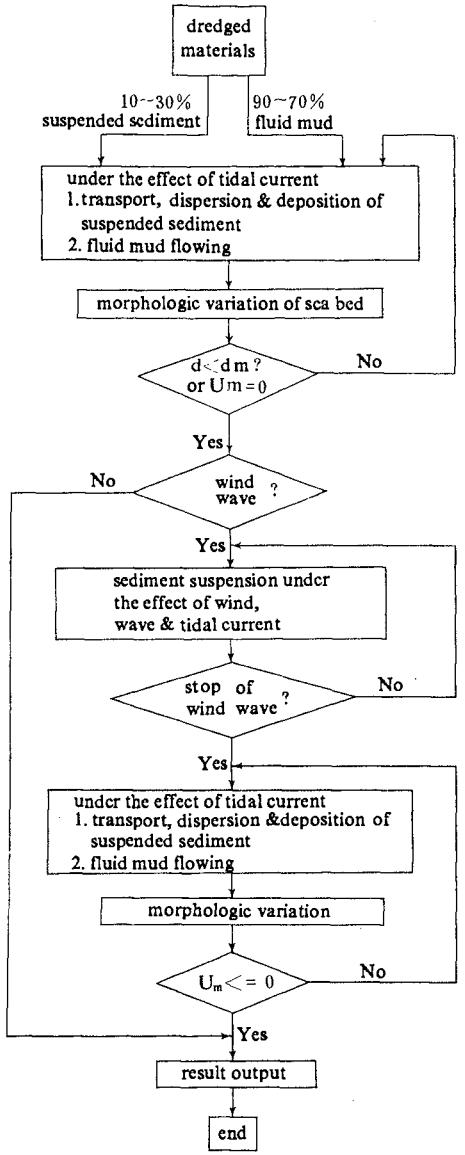

Fig. 1 Diagram of numerical model of dredged materials

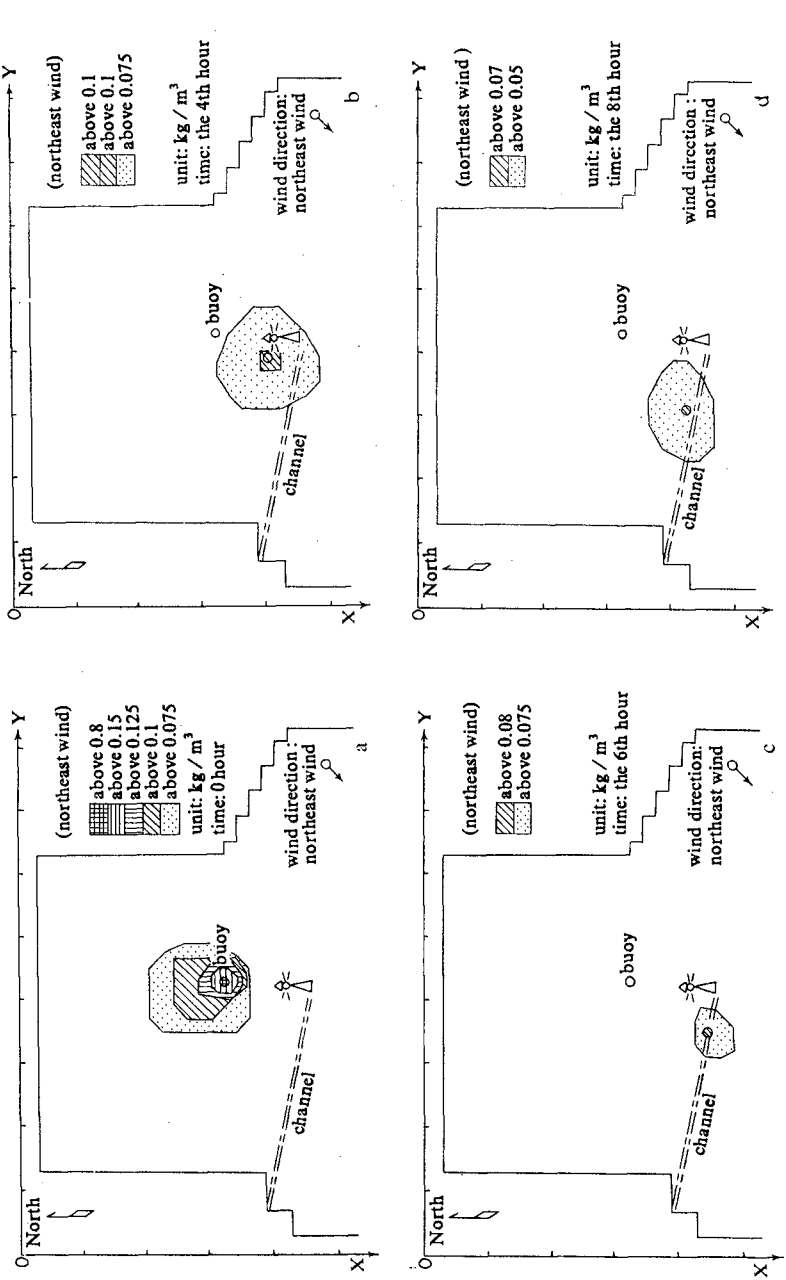

Fig. 2 Diagram of suspended sediment distribution prosesses under the effect of northeast wind

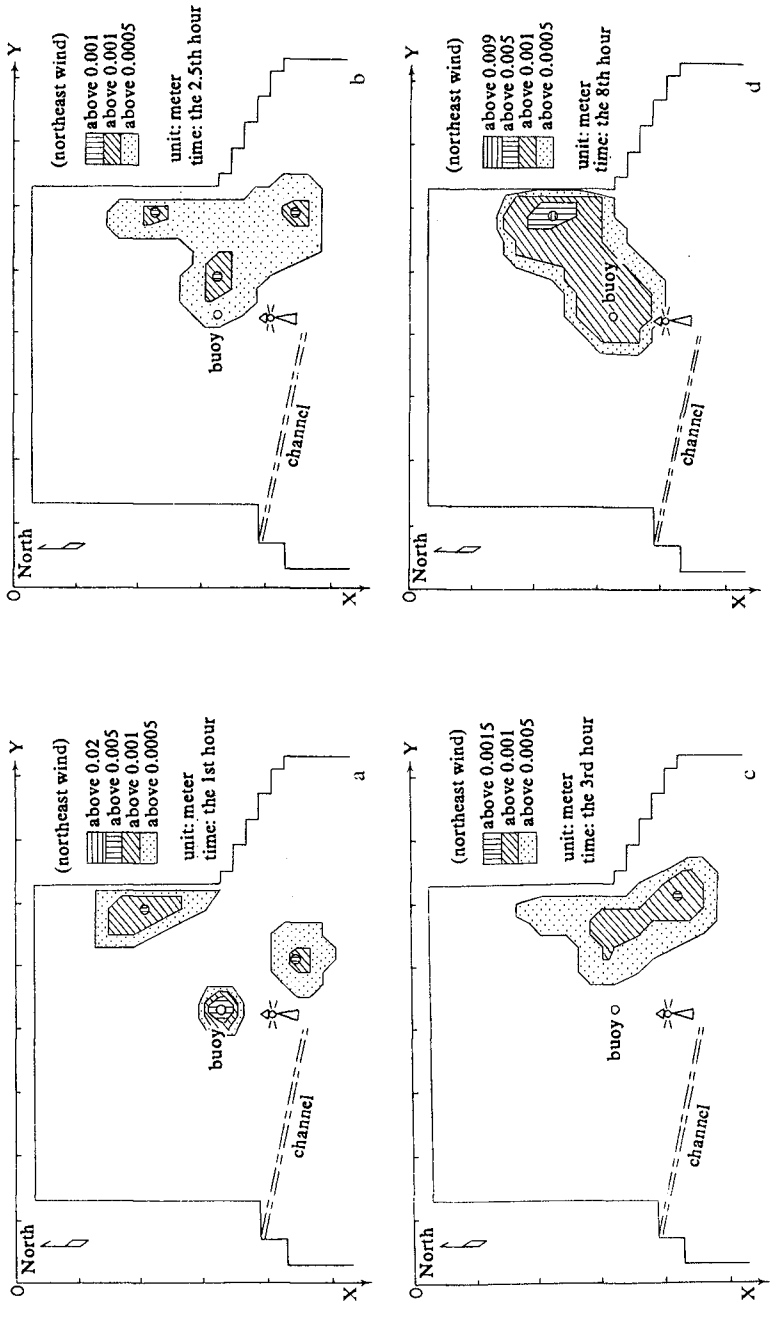

Fig. 3 Diagram of fluid mud distribution processes due to northeast wind